

On convergence of multiscale methods

Axel Målqvist Daniel Peterseim

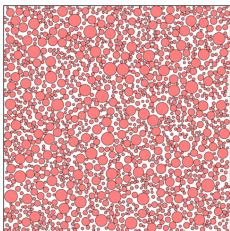
Uppsala University

Humboldt Universität

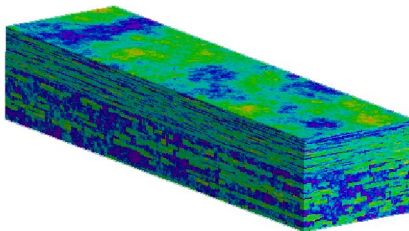
2012-06-26

Multiscale Problems

Applications such as



▷ composite materials



▷ flow in a porous medium

require numerical solution of partial differential equations with rough data (module of elasticity, conductivity, or permeability).

Major challenge: Features on **multiple non-separated scales**.

Multiscale Problems

Oil reservoir simulation



Find pressure p and water concentration s such that:

$$-\nabla \cdot k\mu(s)\nabla p = q, \quad \dot{s} - \nabla \cdot [f(s)\mu(s)k\nabla p] = g,$$

where k is permeability, $\mu(s)$ the total mobility, f fractional flow, and g, q sink and source terms.

Multiscale Problems

Oil reservoir simulation



Find pressure p and water concentration s such that:

$$-\nabla \cdot k \mu(s_n) \nabla p_{n+1} = q, \quad \frac{s_{n+1} - s_n}{\Delta t} - \nabla \cdot [f(s_n) \mu(s_n) k \nabla p_{n+1}] = g,$$

where k is permeability, $\mu(s)$ the total mobility, f fractional flow, and g, q sink and source terms.

Multiscale Problems

Oil reservoir simulation



Find pressure p and water concentration s such that:

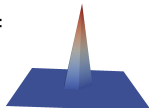
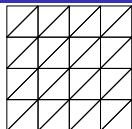
$$-\nabla \cdot k \mu(s_n) \nabla p_{n+1} = q, \quad \frac{s_{n+1} - s_n}{\Delta t} - \nabla \cdot [f(s_n) \mu(s_n) k \nabla p_{n+1}] = g,$$

where k is permeability, $\mu(s)$ the total mobility, f fractional flow, and g, q sink and source terms.

Finite Elements (FE) – Methodology

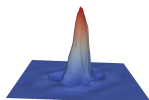
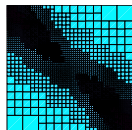
The numerical solution of PDEs by FEM consists of

- construction of an “appropriate” FE mesh
- choosing (local) basis functions (of variable degree of approximation)



An optimal construction should be adapted to the local behavior of the exact solution and, hence, should take into account

- local singularities of the solution (e.g. singularities at re-entrant corners)
- effects of singular perturbations in the solutions (e.g. boundary layers)
- **scales and amplitudes of rough coefficients**



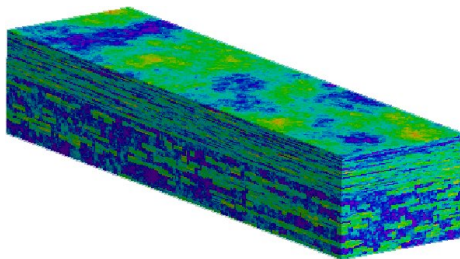
- 1 **Setting and Motivation**
- 2 Multiscale Method and Convergence
- 3 Full Discretization and Numerical Experiments
- 4 Adaptivity
- 5 Conclusion

Model Multiscale Problem

Poisson's equation

$$-\nabla \cdot A \nabla u = f \quad \text{in } \Omega \quad u = 0 \quad \text{on } \partial\Omega$$

with data $f \in L^2(\Omega)$ and $0 < \alpha \leq A \in L^\infty(\Omega)$

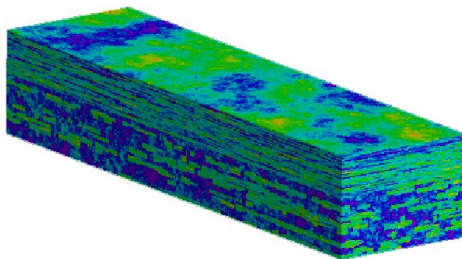


Model Multiscale Problem

Poisson's equation (variational form): $u \in V := H_0^1(\Omega)$ s.t.

$$a(u, v) := \int_{\Omega} (A \nabla u) \cdot \nabla v \, dx = \int_{\Omega} f v \, dx =: F(v) \text{ for all } v \in V$$

with data $f \in L^2(\Omega)$ and $0 < \alpha \leq A \in L^\infty(\Omega)$



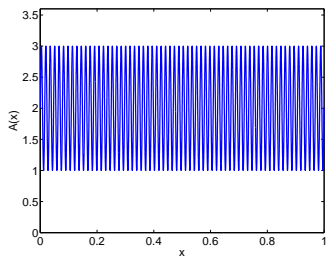
Model Multiscale Problem

Poisson's equation (variational form): $u \in V := H_0^1(\Omega)$ s.t.

$$a(u, v) := \int_{\Omega} (A \nabla u) \cdot \nabla v \, dx = \int_{\Omega} f v \, dx =: F(v) \text{ for all } v \in V$$

with data $f \in L^2(\Omega)$ and $0 < \alpha \leq A \in L^\infty(\Omega)$

Example (periodic coefficient): $A(x) = 2 + \sin(2\pi x/\varepsilon)$, $\varepsilon = 2^{-6}$, $f = 1$



oscillatory coefficient

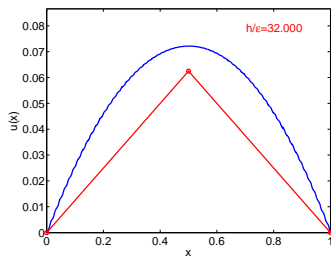
Model Multiscale Problem

Poisson's equation (variational form): $u \in V := H_0^1(\Omega)$ s.t.

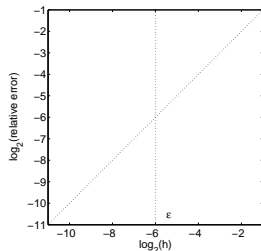
$$a(u, v) := \int_{\Omega} (A \nabla u) \cdot \nabla v \, dx = \int_{\Omega} f v \, dx =: F(v) \text{ for all } v \in V$$

with data $f \in L^2(\Omega)$ and $0 < \alpha \leq A \in L^\infty(\Omega)$

Example (periodic coefficient): $A(x) = 2 + \sin(2\pi x/\varepsilon)$, $\varepsilon = 2^{-6}$, $f = 1$



solution and P1-FEM-approximation



$\log_2(H^1(\Omega) - \text{error})$ vs. $\log_2(h)$

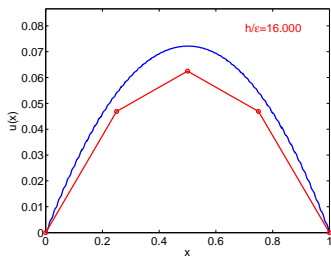
Model Multiscale Problem

Poisson's equation (variational form): $u \in V := H_0^1(\Omega)$ s.t.

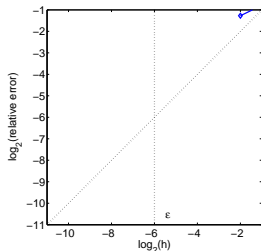
$$a(u, v) := \int_{\Omega} (A \nabla u) \cdot \nabla v \, dx = \int_{\Omega} f v \, dx =: F(v) \text{ for all } v \in V$$

with data $f \in L^2(\Omega)$ and $0 < \alpha \leq A \in L^\infty(\Omega)$

Example (periodic coefficient): $A(x) = 2 + \sin(2\pi x/\varepsilon)$, $\varepsilon = 2^{-6}$, $f = 1$



solution and P1-FEM-approximation



$\log_2(H^1(\Omega) - \text{error})$ vs. $\log_2(h)$

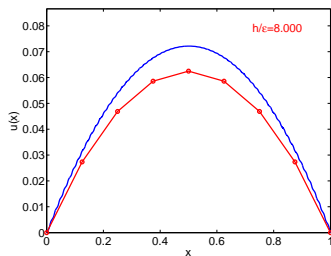
Model Multiscale Problem

Poisson's equation (variational form): $u \in V := H_0^1(\Omega)$ s.t.

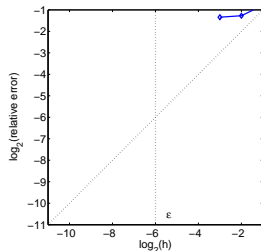
$$a(u, v) := \int_{\Omega} (A \nabla u) \cdot \nabla v \, dx = \int_{\Omega} f v \, dx =: F(v) \text{ for all } v \in V$$

with data $f \in L^2(\Omega)$ and $0 < \alpha \leq A \in L^\infty(\Omega)$

Example (periodic coefficient): $A(x) = 2 + \sin(2\pi x/\varepsilon)$, $\varepsilon = 2^{-6}$, $f = 1$



solution and P1-FEM-approximation



$\log_2(H^1(\Omega) - \text{error})$ vs. $\log_2(h)$

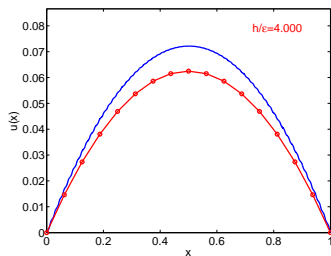
Model Multiscale Problem

Poisson's equation (variational form): $u \in V := H_0^1(\Omega)$ s.t.

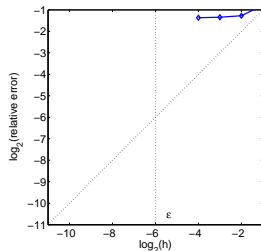
$$a(u, v) := \int_{\Omega} (A \nabla u) \cdot \nabla v \, dx = \int_{\Omega} f v \, dx =: F(v) \text{ for all } v \in V$$

with data $f \in L^2(\Omega)$ and $0 < \alpha \leq A \in L^\infty(\Omega)$

Example (periodic coefficient): $A(x) = 2 + \sin(2\pi x/\varepsilon)$, $\varepsilon = 2^{-6}$, $f = 1$



solution and P1-FEM-approximation



$\log_2(H^1(\Omega) - \text{error})$ vs. $\log_2(h)$

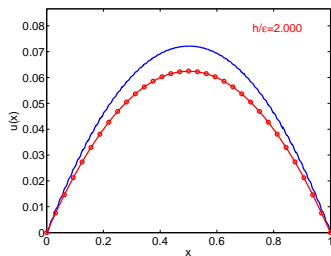
Model Multiscale Problem

Poisson's equation (variational form): $u \in V := H_0^1(\Omega)$ s.t.

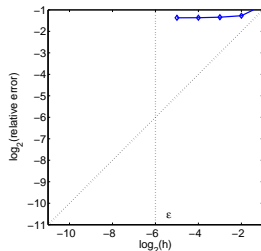
$$a(u, v) := \int_{\Omega} (A \nabla u) \cdot \nabla v \, dx = \int_{\Omega} f v \, dx =: F(v) \text{ for all } v \in V$$

with data $f \in L^2(\Omega)$ and $0 < \alpha \leq A \in L^\infty(\Omega)$

Example (periodic coefficient): $A(x) = 2 + \sin(2\pi x/\varepsilon)$, $\varepsilon = 2^{-6}$, $f = 1$



solution and P1-FEM-approximation



$\log_2(H^1(\Omega) - \text{error})$ vs. $\log_2(h)$

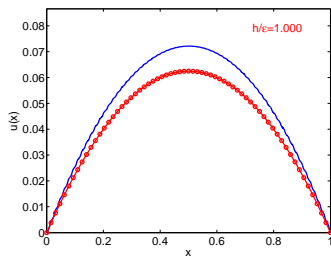
Model Multiscale Problem

Poisson's equation (variational form): $u \in V := H_0^1(\Omega)$ s.t.

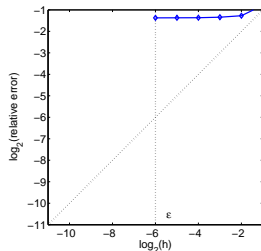
$$a(u, v) := \int_{\Omega} (A \nabla u) \cdot \nabla v \, dx = \int_{\Omega} f v \, dx =: F(v) \text{ for all } v \in V$$

with data $f \in L^2(\Omega)$ and $0 < \alpha \leq A \in L^\infty(\Omega)$

Example (periodic coefficient): $A(x) = 2 + \sin(2\pi x/\varepsilon)$, $\varepsilon = 2^{-6}$, $f = 1$



solution and P1-FEM-approximation



$\log_2(H^1(\Omega) - \text{error})$ vs. $\log_2(h)$

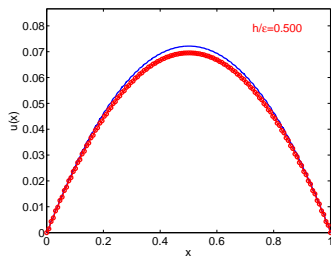
Model Multiscale Problem

Poisson's equation (variational form): $u \in V := H_0^1(\Omega)$ s.t.

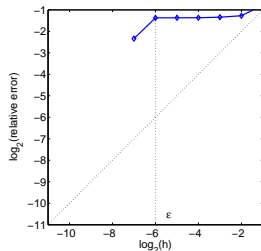
$$a(u, v) := \int_{\Omega} (A \nabla u) \cdot \nabla v \, dx = \int_{\Omega} f v \, dx =: F(v) \text{ for all } v \in V$$

with data $f \in L^2(\Omega)$ and $0 < \alpha \leq A \in L^\infty(\Omega)$

Example (periodic coefficient): $A(x) = 2 + \sin(2\pi x/\varepsilon)$, $\varepsilon = 2^{-6}$, $f = 1$



solution and P1-FEM-approximation



$\log_2(H^1(\Omega) - \text{error})$ vs. $\log_2(h)$

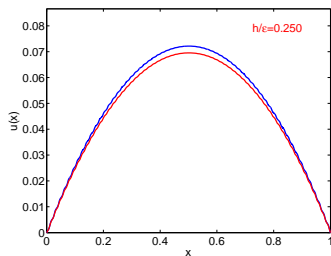
Model Multiscale Problem

Poisson's equation (variational form): $u \in V := H_0^1(\Omega)$ s.t.

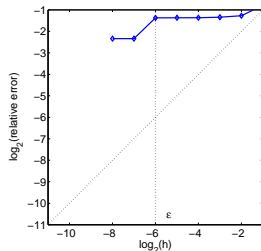
$$a(u, v) := \int_{\Omega} (A \nabla u) \cdot \nabla v \, dx = \int_{\Omega} f v \, dx =: F(v) \text{ for all } v \in V$$

with data $f \in L^2(\Omega)$ and $0 < \alpha \leq A \in L^\infty(\Omega)$

Example (periodic coefficient): $A(x) = 2 + \sin(2\pi x/\varepsilon)$, $\varepsilon = 2^{-6}$, $f = 1$



solution and P1-FEM-approximation



$\log_2(H^1(\Omega) - \text{error})$ vs. $\log_2(h)$

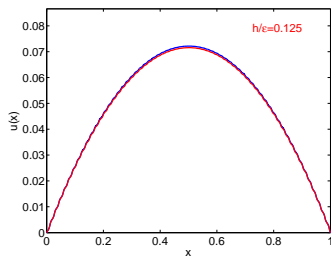
Model Multiscale Problem

Poisson's equation (variational form): $u \in V := H_0^1(\Omega)$ s.t.

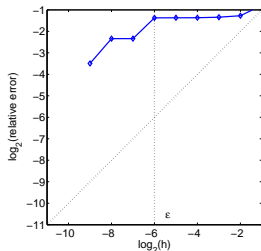
$$a(u, v) := \int_{\Omega} (A \nabla u) \cdot \nabla v \, dx = \int_{\Omega} f v \, dx =: F(v) \text{ for all } v \in V$$

with data $f \in L^2(\Omega)$ and $0 < \alpha \leq A \in L^\infty(\Omega)$

Example (periodic coefficient): $A(x) = 2 + \sin(2\pi x/\varepsilon)$, $\varepsilon = 2^{-6}$, $f = 1$



solution and P1-FEM-approximation



$\log_2(H^1(\Omega) - \text{error})$ vs. $\log_2(h)$

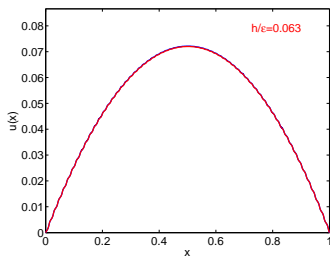
Model Multiscale Problem

Poisson's equation (variational form): $u \in V := H_0^1(\Omega)$ s.t.

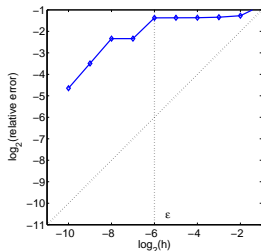
$$a(u, v) := \int_{\Omega} (A \nabla u) \cdot \nabla v \, dx = \int_{\Omega} f v \, dx =: F(v) \text{ for all } v \in V$$

with data $f \in L^2(\Omega)$ and $0 < \alpha \leq A \in L^\infty(\Omega)$

Example (periodic coefficient): $A(x) = 2 + \sin(2\pi x/\varepsilon)$, $\varepsilon = 2^{-6}$, $f = 1$



solution and P1-FEM-approximation



$\log_2(H^1(\Omega) - \text{error})$ vs. $\log_2(h)$

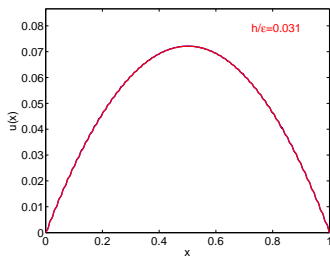
Model Multiscale Problem

Poisson's equation (variational form): $u \in V := H_0^1(\Omega)$ s.t.

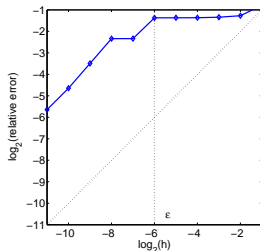
$$a(u, v) := \int_{\Omega} (A \nabla u) \cdot \nabla v \, dx = \int_{\Omega} f v \, dx =: F(v) \text{ for all } v \in V$$

with data $f \in L^2(\Omega)$ and $0 < \alpha \leq A \in L^\infty(\Omega)$

Example (periodic coefficient): $A(x) = 2 + \sin(2\pi x/\varepsilon)$, $\varepsilon = 2^{-6}$, $f = 1$



solution and P1-FEM-approximation



$\log_2(H^1(\Omega) - \text{error})$ vs. $\log_2(h)$

Model Multiscale Problem

Poisson's equation (variational form): $u \in V := H_0^1(\Omega)$ s.t.

$$a(u, v) := \int_{\Omega} (A \nabla u) \cdot \nabla v \, dx = \int_{\Omega} f v \, dx =: F(v) \quad \text{for all } v \in V$$

with data $f \in L^2(\Omega)$ and $0 < \alpha \leq A \in L^\infty(\Omega)$

Examples (periodic coefficients)

- We have $\|u - u_h\| := \|A^{1/2} \nabla(u - u_h)\| \leq C(A, f)h = C'(f)\frac{h}{\epsilon}$.
- We need to resolve the fine scale features even to get the coarse scale behavior right.
- This implies that huge linear systems need to be solved in each time step in the oil reservoir application. Furthermore, the stiffness matrices changes in each time step.

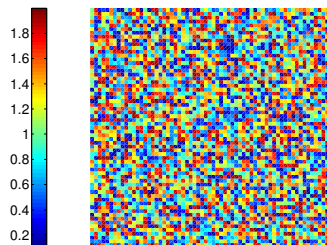
Model Multiscale Problem

Poisson's equation (variational form): $u \in V := H_0^1(\Omega)$ s.t.

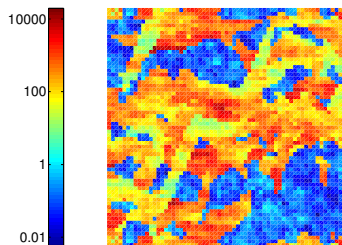
$$a(u, v) := \int_{\Omega} (A \nabla u) \cdot \nabla v \, dx = \int_{\Omega} f v \, dx =: F(v) \text{ for all } v \in V$$

with data $f \in L^2(\Omega)$ and $0 < \alpha \leq A \in L^\infty(\Omega)$

Examples (rough coefficients)



random material (academic)



porous medium (SPE10 benchmark)

Objectives

Without any assumptions on scales ...

- Construction of an upscaled variational problem based on a generalized FEM
(coarse mesh \mathcal{T} of size H & modified nodal basis functions)
- Computation of basis functions involves solution of PDE only on local patches of coarse elements with diameter $\approx \log(1/H)$
- Error estimate

$$\| \| u - u_H^{\text{ms}} \| \| := \| A^{1/2} \nabla (u - u_H^{\text{ms}}) \| \leq C(f) H$$

with $C(f)$ independent of scales of A



A. Målqvist and D. Peterseim.

Localization of Elliptic Multiscale Problems.

ArXiv e-prints, Oct. 2011.

Some Known Methods

- Upscaling techniques: Durlofsky et al. 98, Nielsen et al. 98
- Variational multiscale method: Hughes et al. 95, Arbogast 04, Larson-Målqvist 05, Nolen et al. 08, Nordbotten 09
- Multiscale FEM: Hou-Wu 96, Efendiev-Ginting 04, Aarnes-Lie 06
- Residual free bubbles: Brezzi et al. 98
- Multiscale finite volume method: Jenny et al. 03
- Heterogeneous multiscale method: Engquist-E 03, E-Ming-Zhang 04, Ohlberger 05
- Equation free: Kevrekidis et al. 05
- Metric based upscaling: Owhadi et al. 06
- ...

Common idea

Local approximations (in parallel) on a fine scale are used to modify a coarse scale space or equation

Some Known Methods

- Upscaling techniques: Durlofsky et al. 98, Nielsen et al. 98
- Variational multiscale method: Hughes et al. 95, Arbogast 04, Larson-Målqvist 05, Nolen et al. 08, Nordbotten 09
- Multiscale FEM: Hou-Wu 96, Efendiev-Ginting 04, Aarnes-Lie 06
- Residual free bubbles: Brezzi et al. 98
- Multiscale finite volume method: Jenny et al. 03
- Heterogeneous multiscale method: Engquist-E 03, E-Ming-Zhang 04, Ohlberger 05
- Equation free: Kevrekidis et al. 05
- Metric based upscaling: Owhadi et al. 06
- ...

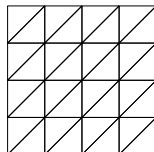
Remark

Error analysis rely on strong assumptions such as scale separation and periodicity

- 1 Setting and Motivation
- 2 **Multiscale Method and Convergence**
- 3 Full Discretization and Numerical Experiments
- 4 Adaptivity
- 5 Conclusion

Multiscale Decomposition

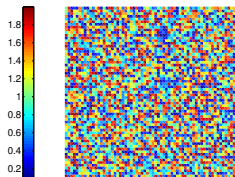
- (coarse) FE mesh \mathcal{T} with parameter H
- P1-FE space $V_H := \{v \in V \mid \forall T \in \mathcal{T}, v|_T \in P_1(T)\}$
- $\mathfrak{I}_{\mathcal{T}} : V \rightarrow V_H$ quasi-interpolation operator



Decomposition

$$V = V_H \oplus V^f \quad \text{with } V^f := \text{kernel } \mathfrak{I}_{\mathcal{T}} = \{v \in V \mid \mathfrak{I}_{\mathcal{T}} v = 0\}$$

Example:



rough coefficient

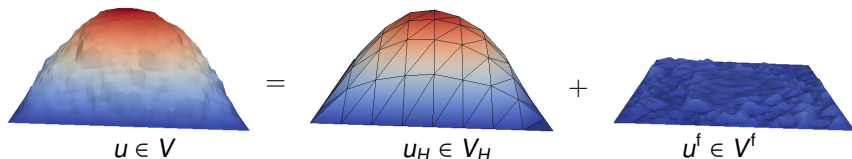
Multiscale Decomposition

- (coarse) FE mesh \mathcal{T} with parameter H
- P1-FE space $V_H := \{v \in V \mid \forall T \in \mathcal{T}, v|_T \in P_1(T)\}$
- $\mathfrak{I}_{\mathcal{T}} : V \rightarrow V_H$ quasi-interpolation operator

Decomposition

$$V = V_H \oplus V^f \quad \text{with } V^f := \text{kernel } \mathfrak{I}_{\mathcal{T}} = \{v \in V \mid \mathfrak{I}_{\mathcal{T}} v = 0\}$$

Example:



Orthogonalization

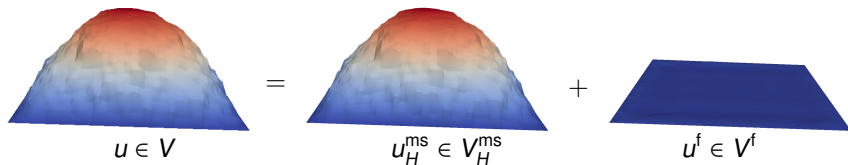
- For each $v \in V_H$ define finescale projection $\mathfrak{F}v \in V^f$ by

$$a(\mathfrak{F}v, w) = a(v, w) \quad \text{for all } w \in V^f$$

Orthogonal Decomposition

$$V = V_H^{\text{ms}} \oplus V^f \quad \text{with } V_H^{\text{ms}} := (V_H - \mathfrak{F}V_H)$$

Example:



Error Analysis (Perfect decomposition)

Lemma

$$\| \|u - u_H^{\text{ms}}\| \| \leq C_{\text{ol}} C_{\mathfrak{T}} \alpha^{-1} \|Hf\|_{L^2(\Omega)}$$

Sketch of proof:

- recall $\|v - \mathfrak{I}_{\mathcal{T}} v\|_{L^2(T)} \leq C_{\mathfrak{T}} H \|\nabla v\|_{L^2(\omega_T)}$ with $\omega_T := \cup\{K \in \mathcal{T} \mid T \cap K \neq \emptyset\}$ [Carstensen/Verfürth '99]
- orthogonal decomposition yields $u^f := u - u_H^{\text{ms}} \in V^f$
- $\mathfrak{I}_{\mathcal{T}} u^f = 0$, interpolation error estimate, and finite overlap of the patches ω_T conclude the proof

$$\begin{aligned} \| \|u^f\| \|^2 &= a(\underbrace{u^f + u_H^{\text{ms}}}_{=u}, u^f) = F(u^f) = F(u^f - \mathfrak{I}_{\mathcal{T}} u^f) \\ &\leq \sum_{T \in \mathcal{T}} \|f\|_{L^2(T)} \|u^f - \mathfrak{I}_{\mathcal{T}} u^f\|_{L^2(T)} \leq C_{\text{ol}} C_{\mathfrak{T}} \alpha^{-1} \|Hf\|_{L^2(\Omega)} \| \|u^f\| \| \quad \square \end{aligned}$$

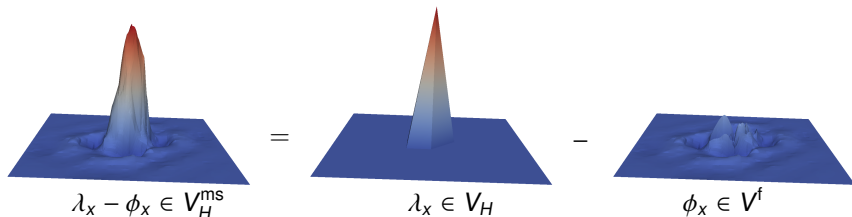
Modified Nodal Basis

- \mathcal{N} denotes set of interior vertices of \mathcal{T}
- $\lambda_x \in V_H$ denotes classical nodal basis function ($x \in \mathcal{N}$)
- $\phi_x = \mathfrak{F}\lambda_x \in V^f$ denotes finescale correction of λ_x ($x \in \mathcal{N}$)

Ideal multiscale FE space

$$V_H^{\text{ms}} = \text{span} \{ \lambda_x - \phi_x \mid x \in \mathcal{N} \}$$

Example



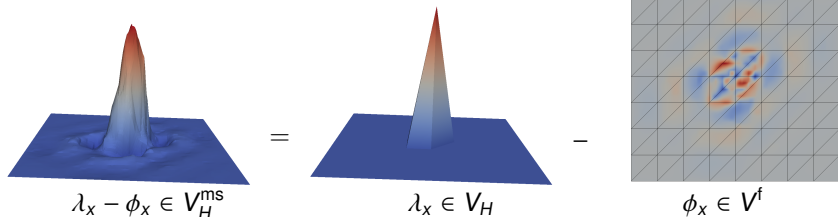
Modified Nodal Basis

- \mathcal{N} denotes set of interior vertices of \mathcal{T}
- $\lambda_x \in V_H$ denotes classical nodal basis function ($x \in \mathcal{N}$)
- $\phi_x = \mathfrak{F}\lambda_x \in V^f$ denotes finescale correction of λ_x ($x \in \mathcal{N}$)

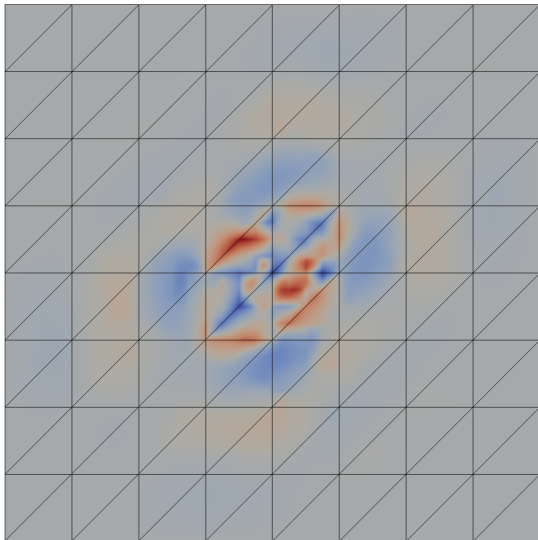
Ideal multiscale FE space

$$V_H^{\text{ms}} = \text{span} \{ \lambda_x - \phi_x \mid x \in \mathcal{N} \}$$

Example



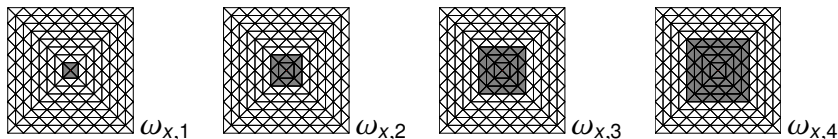
Modified Nodal Basis



Assuming more regularity on A we have $\lambda_x - \phi_x \in H^2(\Omega) \cap H_0^1(\Omega)$.

Localization

- Define nodal patches of k -th order $\omega_{x,k}$ about $x \in \mathcal{N}$



- Localized corrections $\phi_{x,k} \in V^f(\omega_{x,k}) := \{v \in V^f \mid v|_{\Omega \setminus \omega_{x,k}} = 0\}$
solve

$$a(\phi_{x,k}, w) = a(\lambda_x, w) \quad \text{for all } w \in V^f(\omega_{x,k})$$

Localized multiscale FE spaces

$$V_{H,k}^{\text{ms}} = \text{span}\{\lambda_x - \phi_{x,k} \mid x \in \mathcal{N}\}$$

The Multiscale Method

Multiscale approximation seeks $u_{H,k}^{\text{ms}} \in V_{H,k}^{\text{ms}}$ such that

$$a(u_{H,k}^{\text{ms}}, v) = F(v) \quad \text{for all } v \in V_{H,k}^{\text{ms}}$$

Remarks:

- $\dim V_{H,k}^{\text{ms}} = |\mathcal{N}| = \dim V_H$
- basis functions of the multiscale method have local support and are totally independent
- overlap of the supports is proportional to the parameter k
- error analysis suggests $k \approx \log \frac{1}{H}$
- method can take advantage of periodicity

Error Analysis

Lemma (Truncation error)

There exist $C_1 < \infty$ and $\gamma < 1$ independent of x , k , H such that

$$\|\phi_x - \phi_{x,k}\| \leq C_1 \gamma^k \|\phi_x\|.$$

Theorem (Main result)

$$\|u - u_{H,k}^{\text{ms}}\| \leq C_2 \left(k^d \|H^{-1}\|_{L^\infty(\Omega)} \gamma^k \|f\|_{L^2(\Omega)} + \|Hf\|_{L^2(\Omega)} \right)$$

holds with a constant C_2 that does not depend on H , k , f , or u .

Error Analysis

Lemma (Truncation error)

There exist $C_1 < \infty$ and $\gamma < 1$ independent of x , k , H such that

$$\|\phi_x - \phi_{x,k}\| \leq C_1 \gamma^k \|\phi_x\|.$$

Theorem (Main result)

$$\|u - u_{H,k}^{\text{ms}}\| \leq C_2 \left(k^d \|H^{-1}\|_{L^\infty(\Omega)} \gamma^k \|f\|_{L^2(\Omega)} + \|Hf\|_{L^2(\Omega)} \right)$$

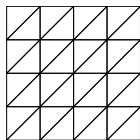
holds with a constant C_2 that does not depend on H , k , f , or u .

Theorem holds without any assumptions on scales or regularity!

- 1 Setting and Motivation
- 2 Multiscale Method and Convergence
- 3 **Full Discretization and Numerical Experiments**
- 4 Adaptivity
- 5 Conclusion

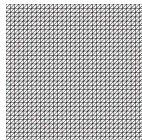
Full Discretization

- Finescale mesh



\mathcal{T}

mesh refinement



\mathcal{T}_h with $h \leq H$

- Reference FE space

$$V_h := \{v \in V \mid \forall T \in \mathcal{T}(\Omega), v|_T \in P_1(T)\}$$

- Reference FE solution $u_h \in V_h$ solves

$$a(u_h, v) = F(v) \quad \text{for all } v \in V_h$$

- Fully discrete corrections $\phi_{x,k}^h \in V_h^f(\omega_{x,k}) := V^f(\omega_{x,k}) \cap V_h$ satisfy

$$a(\phi_{x,k}^h, w) = a(\lambda_x, w) \quad \text{for all } w \in V_h^f(\omega_{x,k})$$

Full Discretization

Fully discrete multiscale FE spaces

$$V_{H,k}^{\text{ms},h} = \text{span}\{\lambda_x - \phi_{x,k}^h \mid x \in \mathcal{N}\}$$

Fully discrete multiscale approximation $u_{H,k}^{\text{ms},h} \in V_{H,k}^{\text{ms},h}$ satisfies

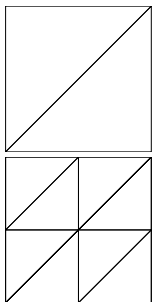
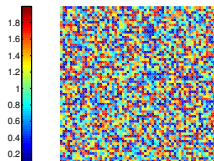
$$a(u_{H,k}^{\text{ms},h}, v) = F(v) \quad \text{for all } v \in V_{H,k}^{\text{ms},h}$$

Theorem (Error estimate)

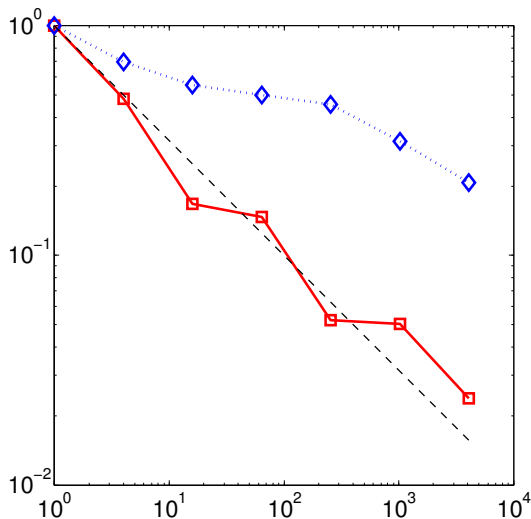
$$\| \| u - u_{H,k}^{\text{ms},h} \| \| \leq C_3 \left(\| \| u - u_h \| \| + k^d \| H^{-1} \|_{L^\infty(\Omega)} \gamma^k \| f \|_{L^2(\Omega)} + \| Hf \|_{L^2(\Omega)} \right)$$

holds with a constant C_3 that does not depend on H , h , k , f , or u .

Numerical Experiment I

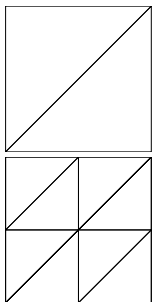
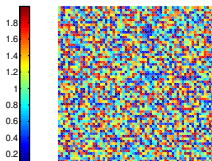


$$H = 2^{-1}, 2^{-2}, \dots, 2^{-7}$$
$$h = 2^{-9}, k = \log(1/H)$$

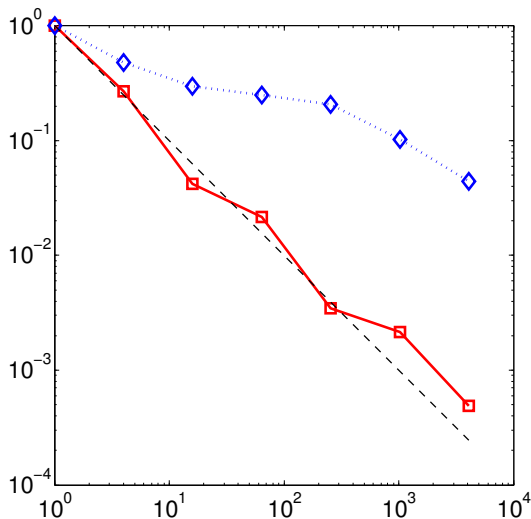


$\|u_h - u_{H,k}^{ms,h}\|$ vs. #dof

Numerical Experiment I

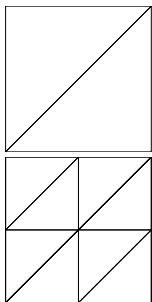
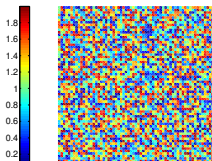


$$H = 2^{-1}, 2^{-2}, \dots, 2^{-7}$$
$$h = 2^{-9}, k = \log(1/H)$$

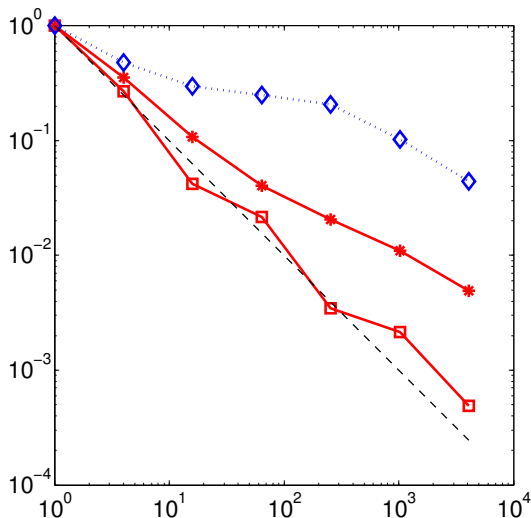


$\|u_h - u_{H,k}^{ms,h}\|$ vs. #dof

Numerical Experiment I

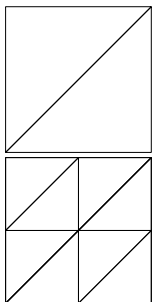
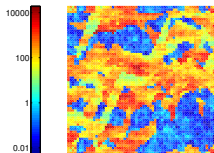


$$H = 2^{-1}, 2^{-2}, \dots, 2^{-7}$$
$$h = 2^{-9}, k = \log(1/H)$$

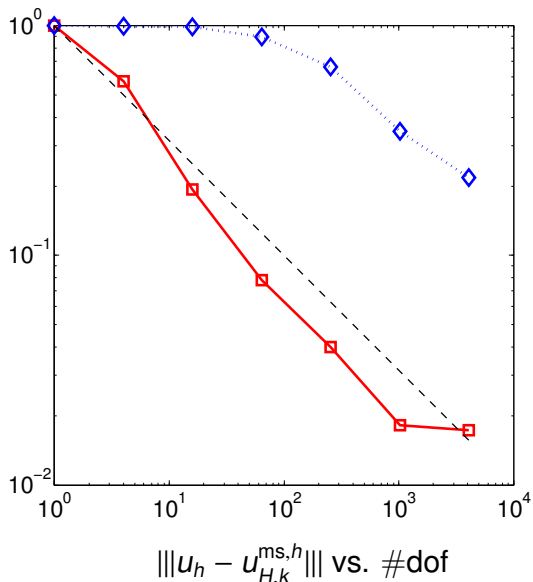


$$\|u_h - \mathfrak{J}_T u_{H,k}^{ms,h}\| \text{ vs. } \#dof$$

Numerical Experiment II

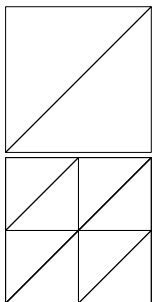
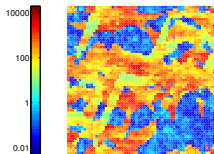


$$H = 2^{-1}, 2^{-2}, \dots, 2^{-7}$$
$$h = 2^{-9}, k = \log(1/H)$$

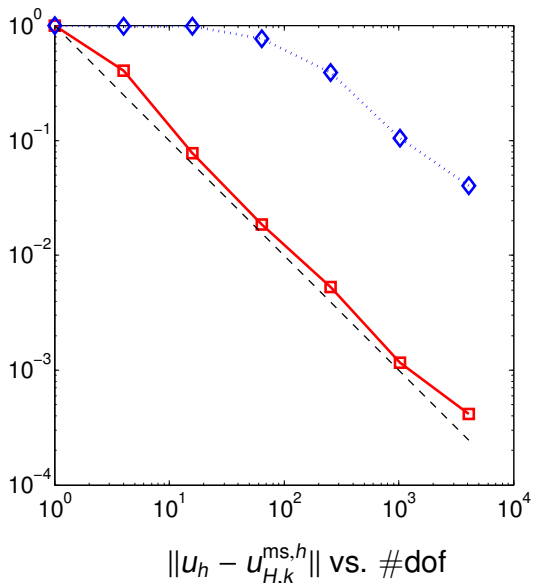


$|||u_h - u_{H,k}^{ms,h}|||$ vs. #dof

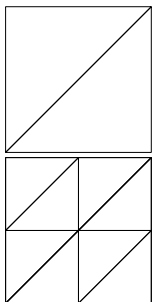
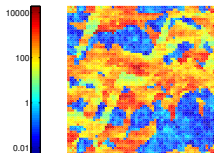
Numerical Experiment II



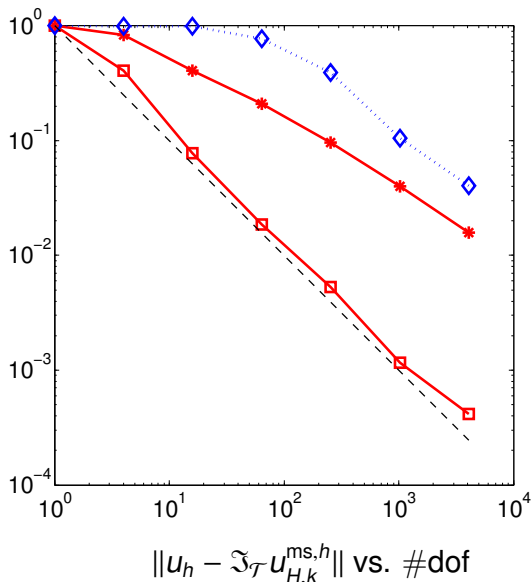
$$H = 2^{-1}, 2^{-2}, \dots, 2^{-7}$$
$$h = 2^{-9}, k = \log(1/H)$$



Numerical Experiment II



$$H = 2^{-1}, 2^{-2}, \dots, 2^{-7}$$
$$h = 2^{-9}, k = \log(1/H)$$



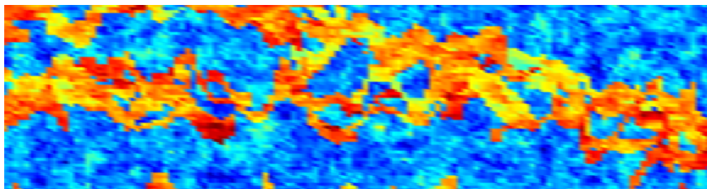
$\|u_h - \mathfrak{F}_{\mathcal{T}} u_{H,k}^{ms,h}\|$ vs. #dof

- 1 Setting and Motivation
- 2 Multiscale Method and Convergence
- 3 Full discretization and Numerical Experiments
- 4 **Adaptivity**
- 5 Conclusion

A posteriori error estimation and adaptivity

Motivation:

- The method we propose will have overlapping patches, which (especially in 3D) is expensive.
- The problems we consider often includes channels so the solution is typically somewhat localized in space.
- The size of the patches and the refinement level is difficult to predict a priori, we therefore need error indicators to tune these parameters automatically.



A posteriori error estimation and adaptivity

Let $\rho^2(v) = \sum_{K \in \mathcal{T}_h} h_K^2 \|\nabla \cdot A \nabla v\|_{L^2(K)}^2 + h_K \|[n \cdot A \nabla v]\|_{L^2(\partial K)}^2$.

Theorem

$$\|u - u_{H,k}^{\text{ms},h}\|^2 \leq C \|Hf\|_{L^2(\Omega)}^2 + C(u_{H,k}^{\text{ms},h}) \sum_{x \in \mathcal{N}} \rho^2(\lambda_x - \phi_{x,k}^h) \\ + C(u_{H,k}^{\text{ms},h}) \sum_{x \in \mathcal{N}} H \|n \cdot A \nabla \phi_{x,k}^h\|_{L^2(\partial \omega_{x,k})}^2$$

- Effect of coarse mesh size included in first term.
- A standard element indicator on each patch measuring the effect of decreasing fine scale mesh size h .
- A new indicator on the boundary of each patch $\partial \omega_{x,k}$. The a priori analysis shows that $\phi_{x,k}^h$ decays exponentially in k .

A posteriori error estimation and adaptivity

Let $\rho^2(v) = \sum_{K \in \mathcal{T}_h} h_K^2 \|\nabla \cdot A \nabla v\|_{L^2(K)}^2 + h_K \|[n \cdot A \nabla v]\|_{L^2(\partial K)}^2$.

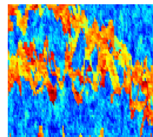
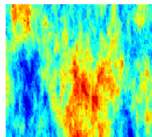
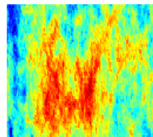
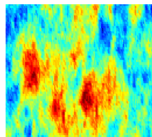
Theorem

$$\|u - u_{H,k}^{\text{ms},h}\|^2 \leq C \|Hf\|_{L^2(\Omega)}^2 + C(u_{H,k}^{\text{ms},h}) \sum_{x \in \mathcal{N}} \rho^2(\lambda_x - \phi_{x,k}^h) \\ + C(u_{H,k}^{\text{ms},h}) \sum_{x \in \mathcal{N}} H \|n \cdot A \nabla \phi_{x,k}^h\|_{L^2(\partial \omega_{x,k})}^2$$

- 1 Compute multiscale approximation, $u_{H,k}^{\text{ms},h}$.
- 2 Compute local error indicators.
- 3 If the error bound is small enough break.
- 4 Otherwise, decrease h locally if interior indicator is large and increase k locally if boundary indicator is large.
- 5 Go back to 1.

Numerical example

- Let the coarse mesh consist of 32×32 elements.
- Let the fine reference mesh consist of 256×256 elements.
- $f = -1$ in lower left corner ($0 \leq x, y \leq 1/128$) and $f = 1$ in upper right corner, otherwise $f = 0$.
- $A =$



We use a symmetric **DG method** as base for the multiscale method. Local problems are solved using **Neumann boundary conditions**, hanging nodes are allowed, there is a common reference mesh.

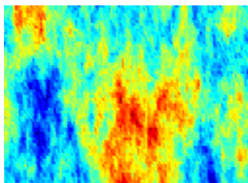


D. Elfverson, E. Georgoulis, and A. Målqvist.

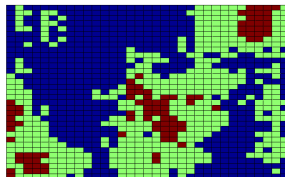
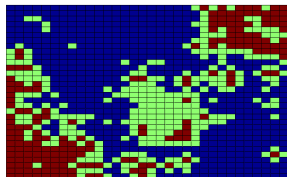
An adaptive discontinuous Galerkin multiscale method for elliptic problems,
Submitted to SIAM MMS.

Numerical example

We start with $h = H/2$ and $k = 2$ in all local problem. In each iteration we refine (divide h by 2) and increase (add 1 to k) 30% of the patches.

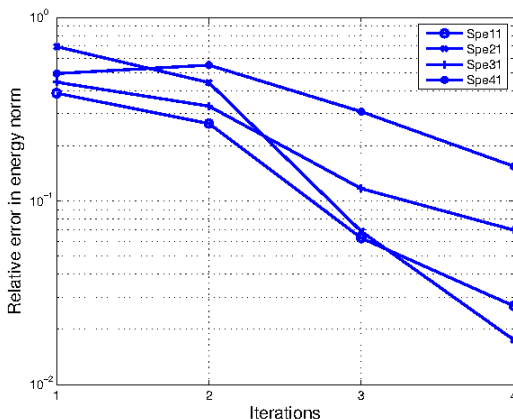


We plot h and k for SPE layer 31 after three iterations.



Numerical example

Convergence of relative error vs. number of iterations.



We note that SPE layer 41 is more difficult, $\max a / \min a \approx 6 \cdot 10^6$ instead of $6 \cdot 10^5$.

Why DG?

Advantage:

- It allows for Neumann conditions on the patches since discontinuous fine scale solutions are not a problem.
- One can use adaptively refined local subgrid and still have a global reference grid by using hanging nodes.
- Construction of a conservative flux, which is essential in the application area, is easy.

Disadvantage:

- Expensive.
- There is a penalty parameter which needs to be tuned.

- 1 Setting and Motivation
- 2 Multiscale Method and Convergence
- 3 Full discretization and Numerical Experiments
- 4 Adaptivity
- 5 **Conclusion**

Conclusion

- A new variational multiscale FEM yields scale-independent textbook convergence and, hence, establishes reliable computational approximation of multiscale problems.
- Numerical experiments confirms the theoretical results. Furthermore numerical results are not sensitive to high contrast.
- An adaptive algorithm for automatic tuning of critical method parameters is presented.
- Numerical examples confirms rapid decrease in error for very challenging permeability coefficients.
- Using multiscale basis functions turn out to be very efficient in the flow in porous media application since basis functions can be reused and are only updated at the front.

Outlook

- Treatment of high contrast also in the analysis, error bound for $\mathfrak{S}_{\mathcal{T}} \mathbf{u}_{H,k}^{\text{ms},h}$, and error bounds in $L^2(\Omega)$ norm.
- Design and analysis of reliable multiscale methods for parabolic and hyperbolic problems.
- Design of a multiscale approach to the full two phase flow system.
- Consider **uncertainty** in the coefficient and construct efficient algorithms for computing statistical information, such as distribution function, of output quantities of interest.
- Consider CO₂ storage applications together with Department of Earth Science at Uppsala University.